Available online at www.sciencedirect.com
ScienceDirect
Geochimica et Cosmochimica Acta 70 (2006) 5634–5650
Geochimica
www.elsevier.com/locate/gca

Spinel group minerals in LL3.00–6 chondrites: Indicators of nebular and parent body processes

M. Kimura [a,*], H. Nakajima [a], H. Hiyagon [b], M.K. Weisberg [c,d]

[a] Faculty of Science, Ibaraki University, Mito 310-8512, Japan
[b] Department of Earth and Planetary Science, Graduate School of Science, The University of Tokyo, 7-3-1, Tokyo 113-0033, Japan
[c] Department of Physical Sciences, Kingsborough College of the City University of New York, Brooklyn, NY 11235, USA
[d] Department of Earth and Planetary Sciences, American Museum of Natural History, New York, NY 10024, USA

Received 30 January 2006; accepted in revised form 17 August 2006

Abstract

We carried out a systematic study of spinel group minerals in LL3.00–3.9 and LL4–6 chondrites. With increasing petrologic type, the size and abundance of spinel increase. The compositions of spinel group minerals in type 3 chondrites depend on the occurrence; Mg–Al-rich spinel occurs mainly in chondrules. Some chromite occurs in chondrules and matrix, and nearly pure chromite is exclusively encountered in the matrix. The occurrence of nearly pure chromite and the wide compositional variations distinguish spinel group minerals in types 3.00–3.3 from those in the other types. Spinel group minerals in types 3.5–3.9 show a narrower range of compositions, and those in types 4–6 are homogeneous. The changes in composition and abundance of spinel in type 3 chondrites are most likely due to thermal metamorphism. Therefore, the chemistry of spinel group minerals could be used as a sensitive indicator of metamorphic conditions, not only for type 3–6, but also 3.00–3.9. They can be applied to identify the most primitive (least metamorphosed) chondrites. The bulk compositions of spinel-bearing chondrules and the textural setting of the spinel indicate that most spinel group minerals crystallized directly from chondrule melts. However, some spinel grains, especially those enclosed in olivine phenocrysts, can not be explained by *in situ* crystallization in the chondrule. We interpret these spinel grains to be relic phases that survived chondrule melting. This is supported by the oxygen isotopic composition of a spinel grain, which has significantly lighter oxygen than the coexisting olivine. The oxygen isotopic composition of this spinel is similar to those of Al-rich chondrules. Our discovery of relic spinel in chondrules is an indication of the complexities in the early solar nebular processes that ranged from formation of refractory inclusion, through Al-rich chondrule, to ferromagnesian chondrules, and attests to the recycling of earlier formed materials into the precursors of later formed materials. The characteristic features of spinel group minerals are not only sensitive to thermal metamorphism, but also shed light on chondrule formation processes.

1. Introduction

Ordinary chondrites are classified into petrologic types 3–6, based on their texture and mineralogy (Van Schmus and Wood, 1967). The petrologic type reflects the degree of thermal metamorphism that the meteorite experienced in the parent body. Type 3 chondrites (unequilibrated chondrites) are further subdivided into types 3.0–3.9 based on their thermoluminescence sensitivity (Sears et al., 1980). The sensitivity of ordinary chondrites is dependent on the degree of crystallization of the chondrule mesostasis, which ranges from pure glass in type 3.0 chondrites to more crystalline in higher petrologic types.

Chondrites of the lower petrologic types, especially 3.0, are important because they are the most likely to preserve primordial petrologic, chemical and isotopic features important for deciphering nebular processes (e.g., Brearley and Jones, 1998; Kita et al., 2000). Therefore, several petrologic and mineralogical criteria, such as chemical homogeneity of silicate minerals (e.g., Sears and Dodd, 1988), have been applied to classify the petrologic type 3.0–3.9

* Corresponding author. Fax: +81 292 28 8388.
E-mail address: makotoki@mx.ibaraki.ac.jp (M. Kimura).

0016-7037/$ - see front matter © 2006 Elsevier Inc. All rights reserved.
doi:10.1016/j.gca.2006.08.023

chondrites and identify the most pristine and least equilibrated varieties.

However, mineralogical criteria for distinguishing the lower petrologic types, especially lower than 3.5, are not well established. On the other hand, Grossman and Brearley (2005) recently showed that the distribution of Cr in olivine changes systematically with increasing degree of thermal metamorphism. They proposed that Cr distribution in olivine can be used to subdivide petrologic types 3.0–3.1 into 3.00 through 3.15.

It is well known that the chemical compositions of spinel group minerals can be used to distinguish chemical groups and petrologic types 3–6 in ordinary chondrites (e.g., Bunch et al., 1967; Yabuki et al., 1983; Johnson and Prinz, 1991). Although Nehru et al. (1997) showed that there is no clear correlation between petrologic type and chromite compositions in H3.4–3.8, L3.3–3.8 and LL3.0–3.8 chondrites, preliminary works of Kimura (2000) and Tomiyama et al. (2001) showed that the compositions of spinel group minerals are related to petrologic type in unequilibrated ordinary chondrites.

Here we report the results of our systematic study of spinel group minerals in LL3–6 chondrites. We found that spinel group minerals are commonly present in all LL chondrites, and that spinel chemistry is a good indicator of petrologic type and metamorphic conditions even in ordinary chondrites of lower types.

We also found that some chondrites contain relic spinel that formed before chondrule melting. We present the petrologic, chemical and oxygen isotopic compositions of these spinel grains and argue that they preserve primary features that survived chondrule formation. Thus, the features of spinel group minerals in ordinary chondrites reflect not only the effects of parent body thermal metamorphism, but also nebular processes. Preliminary results were reported in Kimura et al. (2003).

2. Samples and experimental methods

We investigated polished thin sections of 11 LL chondrites, which were selected from the meteorite collections of the National Institute of Polar Research (NIPR), and the American Museum of Natural History (AMNH), except for Bo Xian from the Guangzhou Institute of Geochemistry.

Back-scattered electron (BSE) imaging and mineral analyses were obtained using the JEOL 733 electron-probe microanalyzer (EPMA) at Ibaraki University. Quantitative mineral analyses were conducted generally at 15 kV and a sample current of 30 nA. The X-ray overlaps of K_β on K_α lines of some successive elements were corrected with a deconvolution program. The standard ZAF matrix correction method was used for spinel group minerals, in order to measure Zn and V with lower detection limits. The Bence-Albee correction method was used for silicate phases. The bulk compositions of some spinel-bearing chondrules were also measured with broad beam EPMA, and corrected by the method after Ikeda (1980). The detection limits of EPMA analyses in this study are shown in Tables 2–5.

We measured the areas occupied by spinel grains and the area of the entire section. From these data, we calculated the modal abundances of spinel group minerals.

The oxygen isotopic compositions of spinel and the coexisting phases in chondrules were measured using a CAMECA ims-6f ion microprobe at the University of Tokyo, after the method of Hiyagon and Hashimoto (1999). In the measurements of oxygen isotopic compositions, experimental errors are 1σ. There is no matrix effect between olivine and spinel within analytical uncertainties (<2‰), and no correction was made for the spinel oxygen isotopic data.

3. Results

3.1. Occurrence of spinel group minerals in LL chondrites

Table 1 shows the list of 11 samples studied here, eight LL3 (3.00–3.9) and three LL4–6 chondrites. We applied the classification criteria proposed by Grossman and Brearley (2005), and reclassified Y-74660 (LL3.0 by NIPR) into LL3.15, since the average Cr_2O_3 content and the standard deviation in olivine are 0.24% and 0.21%, respectively.

Table 1
Samples and occurrences of spinel group minerals

Class	Meteorite	Section	Area (mm^2)[a]	Size (μm)[b]	Abundance (vol%)[c]
LL3.00	Semarkona	AMNH 4128-3	120.0	17.2 ± 17.2	0.01
LL3.15	Y-74660	NIPR 81-2	46.3	11.4 ± 6.4	0.01
LL3.2	Krymka	AMNH 4847-1	182.0	13.2 ± 11.8	0.01
LL3.2	Y-790448	NIPR 91-6	24.3	12.5 ± 11.3	0.14
LL3.3	Wells	AMNH 4928-2	171.0	29.5 ± 24.7	0.02
LL3.5	ALHA77260	NIPR 71-3	41.1	11.3 ± 6.4	0.03
LL3.7	ALHA77304	NIPR 83-3	58.2	15.0 ± 10.2	0.04
LL3.9	Bo Xian	GIG	207.3	11.1 ± 10.0	0.01
LL4	Y-74002	NIPR 95-3	54.5	32.4 ± 30.1	0.24
LL5	Y-74022	NIPR 92-3	29.6	36.6 ± 29.3	0.41
LL6	Y-790256	NIPR 74-2	53.4	44.5 ± 29.4	0.48

[a] Area of thin section studied here.
[b] Average and standard deviation of apparent size of spinel group minerals.
[c] Modal abundance of spinel group minerals.

We performed EPMA mapping in order to count all spinel grains from sections, and found that all these samples contain spinel group minerals more than a few μm in size. Besides spinel, ilmenite is commonly present in all samples studied, and rutile, perovskite and an unknown Zr–Al-oxide rarely occur in the LL3.00–3.3 chondrites studied here (Kimura et al., 2004).

Although spinel group minerals show a wide range of occurrences in type 3 chondrites, they can be summarized as follows: (1) as isolated minerals in the fine-grained opaque matrix (Fig. 1a), (2) in intimate association with coarse Fe–Ni metal and troilite grains, mostly in the matrix (Fig. 1b), (3) among phenocrysts in chondrules (Figs. 1c and d), and (4) as inclusion in olivine phenocrysts in chondrules (Fig. 1e).

Spinel group minerals in occurrences 1 and 2 commonly show anhedral to subhedral form. In occurrence 3, the spinel is usually euhedral to subhedral in form, and is associated with olivine and pyroxene phenocrysts, and within the groundmass glass. Spinel enclosed in olivine phenocrysts (occurrence 4) is always irregular to spherical in shape.

In LL3.00–3.5 chondrites, 70–80% of all spinel grains occur in chondrules (occurrences 3 and 4), whereas in ALHA77304 (LL3.7) it is ~50%. In Bo Xian (LL3.9), spinel group minerals associated with opaque phases (occurrence 2) is the most common occurrence (~70%), and only ~20% of the spinel grains are present in chondrules. In LL4–6 chondrites as is well known, spinel group minerals are present in chondrules and matrix, typically as anhedral grains (Fig. 1f).

The shock degrees of all the samples we studied are lower than S3. Rubin (2003) showed that chromite is associated with plagioclase in shocked chondrites. This occurrence of chromite was not observed in the samples studied here. Chromitic chondrules (e.g., Krot et al., 1993) were also not encountered in the samples we studied.

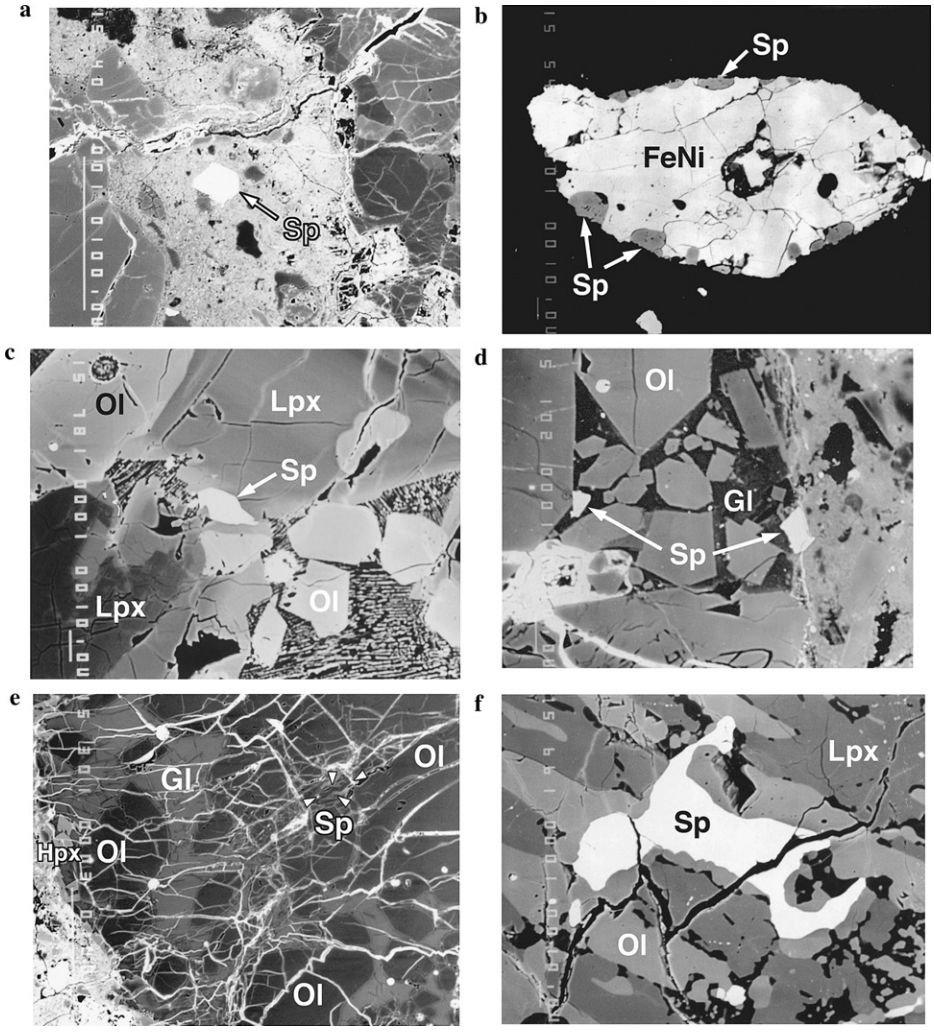

Fig. 1. Back-scattered electron (BSE) images of spinel group minerals. (a) Isolated spinel group mineral (Sp) in the fine-grained opaque matrix in Wells (LL3.3). Width is 250 μm; (b) Spinel group minerals in close association with Fe–Ni metal (Fe–Ni) in the matrix in Bo Xian (LL3.9). Width is 220 μm; (c) Spinel among phenocrystic low-Ca pyroxene (Lpx) and olivine (Ol) in a chondrule of Y-74660 (LL3.15). Width is 130 μm; (d) Spinel in groundmass glass (Gl) in a chondrule from ALHA77260 (LL3.5). Width is 90 μm; (e) Spinel as an inclusion in an olivine phenocryst in a chondrule from Wells (LL3.3). The boundary of the spinel grain is shown by triangles. Width is 400 μm; (f) Spinel group mineral in a chondrule from Y-74022 (LL5). Width is 180 μm.

Table 1 shows the average apparent size distribution of spinel group minerals in LL3–6 chondrites. We define the size by the average of the longest and shortest dimensions of each grain. The average size in LL3.00–3.9 ranges from 11 to 17 μm, except in Wells (~30 μm), whereas it increases in LL4 to LL6, from 32 to 45 μm. Table 1 also shows the standard deviation of the size distribution. The deviation does not seem to decrease or increase consistently with type. However, the standard deviations for spinel grain size are consistently greater in LL4–6 than in the L3 chondrites we studied. The range of size is large even in type 6 chondrites and size varies continuously from fine to coarse grains. The size difference between spinel grains in type 3 and 4 chondrites was also noted in Bridges et al. (2004).

The size distribution does not seem to depend on the textural occurrence; e.g., in Y-74660, 8–34 μm (12 μm in average) is the size range for spinel group minerals in the matrix, and 4–23 μm (11 μm) is the range for spinel in the chondrules. Only in Bo Xian, spinel group minerals associated with opaque minerals are smaller in size, mostly <10 μm, than the others, which are ~15 μm.

The modal abundance of spinel in LL3.0–3.9 ranges from 0.01 to 0.04 vol%, except in Y-790448 (LL3.2) (0.14%). The sample of Y-790448 that we studied contains a large chondrule bearing high amounts of spinel with rare perovskite (Kimura et al., 2004). Spinel abundance appears to increase from LL4 to LL6 (0.2 to 0.5 vol%), based on the limited number of chondrites that we studied. Keil (1962) measured the modal abundances of chromite in LL6 chondrites by point-counting. He reported ~0.2 vol% chromite in LL6 chondrites. Gastineau-Lyons et al. (2002) also measured the modal compositions of ordinary chondrites by X-ray spectra and found that the abundance of chromite ranges from 0.6 to 0.9 vol% in LL4–6 chondrites. Although the absolute values of spinel abundance seem to vary depending on the technique used to measure it, the general trend of increase in spinel abundance with petrologic type is consistent with our results.

3.2. Mineral chemistry

3.2.1. Major element compositions of spinel group minerals in LL chondrites

Spinel group minerals show a wide compositional variation of solid solutions, and consist of many end members (Deer et al., 1992). Table 2 gives selected analyses of the spinel group minerals in the samples we studied. They are mainly solid solutions of chromite ($FeCr_2O_4$) to spinel ($MgAl_2O_4$), as is well known (e.g., Bunch et al., 1967; Johnson and Prinz, 1991). Since the spinel data are essentially stoichiometric in composition, ferric iron (magnetite component) is negligibly low.

Spinel group minerals can be characterized by their atomic Al/(Al + Cr) ratios (hereafter *al*#) and their Mg/(Mg + Fe) ratios (hereafter *mg*#). Several terminologies have been used for spinel group minerals in chondrites. Johnson and Prinz (1991) used the term chromite for a wide range of spinel compositions (*al*# ranges 0–0.6). Krot et al. (1993) defined spinel (>0.8 *al*#), chromitic spinel, spinelian chromite and chromite (<0.2 *al*#). According to Wlotzka (2005), Cr-spinel has a wide compositional variation, whereas chromite is homogeneous in equilibrated chondrites.

Fig. 2 shows the compositional distribution, on plots of *mg*# vs. *al*#, in the spinel from the LL3–6 chondrites studied. The *mg*# varies from 0.006 to 0.995, and the *al*# is 0.001–0.995, ranging from nearly pure chromite to nearly pure spinel. However, there are two compositional gaps between the end members of chromite and spinel in LL3.00–3.3 chondrites. Thus, in this paper we divide the spinel group minerals into chromite with $\leqslant$0.2 *mg*# and $\leqslant$0.2 *al*#, and MgAl-spinel with $\geqslant$0.8 *mg*# and $\geqslant$0.8 *al*#. The other spinel group minerals are called Cr-spinel, which generally have intermediate compositions between chromite and MgAl-spinel. LL3.00–3.15 and 3.2–3.3 chondrites have MgAl-spinel, Cr-spinel and chromite, whereas LL3.5–3.9 chondrites contain Cr-spinel and chromite.

In Semarkona (LL3.00), nearly pure MgAl-spinel (>0.98 *mg*# and *al*#) is present (Fig. 2), and such spinel was not found in the other LL chondrite. However, the compositions of spinel group minerals in the most primitive chondrites, LL3.00–3.15 (Fig. 2a), overlap with the compositions of spinel in LL3.2–3.3 (Fig. 2b). The *mg*# and *al*# range from 0.006 to 0.995 (0.365 on average) and 0.001–0.995 (0.388) in LL3.00–3.3, 0.039–0.606 (0.128), and 0.001–0.995 (0.157) in LL3.5–3.9, and 0.071–0.128 (0.094), and 0.125–0.166 (0.137) in LL4–6. The range of compositions generally decrease in the higher petrologic types.

Thus, the compositional variation of spinel group minerals in LL3.00–3.3 chondrites is wider than that in LL3.5–3.9 chondrites. The compositional variation of spinel in LL3.5 is wider than those in LL3.7 and 3.9 chondrites (Table 3 and Fig. 2c). Table 3 shows the average composition and standard deviation of all spinel group minerals in each of the samples studied here. With increasing petrologic type, the standard deviations of major elements, such as Cr_2O_3 and MgO, in the spinel generally decrease, as might be expected. These observations suggest that the chemical compositions of spinel group minerals are related to petrologic type 3.00 to 3.9.

MgAl-spinel, Cr-spinel, and chromite occur in LL3 chondrites. However, the LL4-6 chondrites studied here contain only homogeneous chromite, typical of LL chondrites (Bunch et al., 1967), although Cr-spinel has been reported in some equilibrated chondrites (e.g., Yabuki et al., 1983; McCoy et al., 1991a).

Table 3 also summarizes the average compositions and standard deviations of the spinel group minerals in chondrules and matrix in the samples, respectively. The compositions of spinel group minerals depend on the textural occurrence, especially in chondrites of lower petrologic type. MgAl-spinel and Cr-spinel, with large chemical heterogeneity (Table 3), always occur in the groundmass and in

Table 2
Selected analytical data of spinel group minerals

Sample	Class	Occ.[a]	SiO_2	TiO_2	Al_2O_3	Cr_2O_3	V_2O_3	FeO	MnO	MgO	ZnO	Total	Si[b]	Ti	Al	Cr	V	Fe	Mn	Mg	Zn	Total
Semarkona	LL3.00	C	0.14	0.72	48.15	19.33	0.12	15.28	0.28	15.87	b.d.	99.91	0.004	0.015	1.552	0.418	0.003	0.350	0.007	0.647		2.995
		C	0.18	0.25	70.32	0.56	0.32	0.27	b.d.	27.82	b.d.	99.71	0.004	0.005	1.976	0.011	0.006	0.005		0.988		2.995
		M	0.34	0.41	0.04	65.99	0.69	32.30	0.75	0.29	b.d.	100.81	0.013	0.011	0.002	1.923	0.020	0.995	0.023	0.016		3.004
		O	0.24	0.13	0.04	66.84	0.89	30.88	1.59	0.17	b.d.	100.77	0.009	0.004	0.002	1.948	0.026	0.952	0.050	0.009		3.000
Y-74660	LL3.15	C	0.15	0.30	43.80	24.80	0.18	15.20	0.21	15.62	b.d.	100.25	0.004	0.006	1.434	0.545	0.004	0.353	0.005	0.647		2.998
		C	0.34	0.89	22.55	42.50	0.27	24.00	0.55	7.81	b.d.	98.91	0.011	0.022	0.852	1.077	0.007	0.643	0.015	0.373		3.000
		M	0.43	1.08	0.17	62.46	0.98	32.68	0.33	0.71	0.16	99.00	0.016	0.030	0.007	1.849	0.029	1.023	0.010	0.040	0.004	3.010
		O	0.17	4.05	0.19	58.89	0.87	33.82	0.32	0.76	0.26	99.33	0.006	0.113	0.008	1.732	0.026	1.052	0.010	0.042	0.007	2.997
Krymka	LL3.2	C(R)	0.16	0.22	64.81	4.45	0.24	7.50	b.d.	22.63	0.13	100.14	0.004	0.004	1.899	0.088	0.005	0.156		0.839	0.002	2.996
		C	0.34	1.45	1.41	62.17	0.83	32.74	0.31	0.79	0.24	100.27	0.013	0.040	0.061	1.803	0.024	1.004	0.010	0.043	0.006	3.004
		O	0.16	0.45	b.d.	66.95	0.53	31.19	0.31	0.34	0.28	100.22	0.006	0.013		1.959	0.016	0.965	0.010	0.019	0.008	2.994
Y-790448	LL3.2	C	0.18	0.46	19.99	48.20	0.39	21.01	0.24	9.76	b.d.	100.21	0.006	0.011	0.746	1.207	0.010	0.556	0.007	0.460		3.002
		C	0.20	0.62	15.41	49.74	0.25	28.37	0.36	3.87	0.20	99.04	0.007	0.016	0.617	1.335	0.007	0.805	0.010	0.196	0.005	2.998
		O	0.25	2.10	0.09	61.87	0.76	32.56	0.49	0.52	0.27	98.91	0.009	0.059	0.004	1.834	0.023	1.020	0.016	0.029	0.007	3.001
Wells	LL3.3	C(R)	0.25	0.29	69.75	0.62	0.17	1.24	b.d.	27.58	b.d.	99.90	0.006	0.005	1.965	0.012	0.003	0.025		0.983		2.999
		C	0.18	0.61	21.88	45.97	0.45	22.11	0.26	8.95	b.d.	100.40	0.006	0.015	0.812	1.144	0.011	0.582	0.007	0.420		2.996
		M	0.22	0.16	b.d.	67.32	0.73	31.43	0.62	0.31	b.d.	100.79	0.008	0.004		1.959	0.022	0.968	0.019	0.017		2.997
ALHA77260	LL3.5	C	0.10	0.36	29.89	37.09	0.31	22.85	0.26	8.61	0.67	100.15	0.003	0.008	1.079	0.898	0.008	0.585	0.007	0.393	0.015	2.996
		O	0.18	1.59	0.36	63.75	0.81	31.04	0.56	0.98	0.25	99.52	0.007	0.044	0.016	1.866	0.024	0.961	0.018	0.054	0.007	2.996
ALHA77304	LL3.7	C	0.06	1.11	4.69	59.85	0.70	30.26	0.61	1.87	0.49	99.63	0.002	0.030	0.199	1.707	0.020	0.913	0.019	0.101	0.013	3.004
		M	0.15	1.32	3.86	60.48	0.76	30.00	0.68	1.58	0.44	99.27	0.005	0.036	0.165	1.737	0.022	0.912	0.021	0.086	0.012	2.996
Bo Xian	LL3.9	C	0.07	2.13	2.87	59.88	0.95	30.85	0.68	1.94	0.39	99.74	0.002	0.058	0.123	1.720	0.028	0.937	0.021	0.105	0.010	3.004
		O	0.08	2.30	2.52	60.99	0.98	30.21	0.62	1.85	0.40	99.95	0.003	0.063	0.107	1.747	0.028	0.915	0.019	0.100	0.011	2.993
Y-74002	LL4	M	0.03	2.05	5.97	57.58	0.79	31.27	0.63	1.65	0.47	100.44	0.001	0.055	0.250	1.620	0.023	0.930	0.019	0.088	0.012	2.998
Y-74022	LL5	M	0.05	1.94	6.63	56.69	0.77	31.44	0.63	1.69	0.28	100.11	0.002	0.052	0.278	1.595	0.022	0.935	0.019	0.090	0.007	2.999
Y-790256	LL6	M	0.06	4.26	5.52	53.81	0.69	32.79	0.60	1.73	0.26	99.72	0.002	0.115	0.233	1.525	0.020	0.983	0.018	0.092	0.007	2.994

b.d., below detection limits (3σ, in wt%), 0.03 for SiO_2, V_2O_3 and Cr_2O_3, 0.04 for Al_2O_3 and MgO, 0.05 for TiO_2 and MnO, 0.07 for FeO, and 0.10 for ZnO.

[a] Occurrence: C, in chondrule; (R), relic grain; M, isolated grain in matrix; O, with opaque minerals in matrix.

[b] Atomic ratio is based on 4 oxygens.

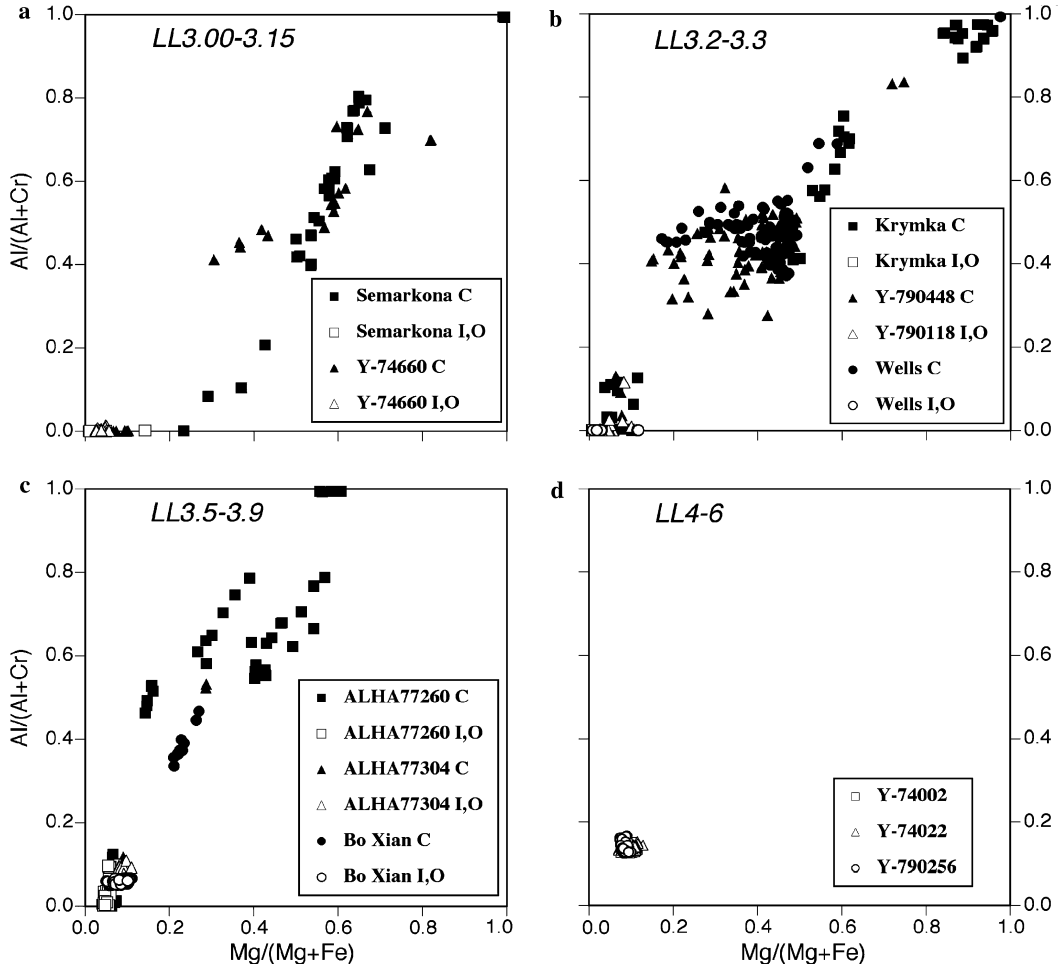

Fig. 2. Atomic Mg/(Mg + Fe) vs. Al/(Al + Cr) ratios of spinel group minerals in (a) Semarkona (LL3.00) and Y-74660 (LL3.15), (b) Krymka (LL3.2), Y-790448 (LL3.2), and Wells (LL3.3), (c) ALHA77260 (LL3.5), ALHA77304 (LL3.7), and Bo Xian (LL3.9), and (d) Y-74002 (LL4), Y-74022 (LL5) and Y-790256 (LL6). C, occurring in chondrule; I, as isolated mineral; and O, intimate association with opaque minerals in the matrix. It is noted that with increasing types (3.00–3.9) the composition becomes homogeneous, and that nearly pure chromite is encountered in type 3.00–3.3 chondrites.

olivine phenocrysts in chondrules (Figs. 1c–e), and never coexists with chromite in the same chondrule. These spinel grains, especially euhedral to subhedral in form, often show chemical zoning from Mg and Cr-rich cores to Fe and Al-rich rims, e.g., *mg*# and *al*# of 0.48 and 0.48 in the cores to 0.26 and 0.54 in the rims, respectively. Chromite typically occurs as isolated minerals within the matrix (Fig. 1a), and associated with Fe–Ni metal and troilite in the matrix (Fig. 1b). Especially, in LL3.00–3.3 chondrites, nearly pure chromite ($<$0.04 *mg*# and *al*#) is found in the matrices generally associated with opaque minerals. Such chromite is never present in chondrites of type $\geqslant$3.5 (Fig. 2).

3.2.2. Minor element compositions of spinel group minerals in LL chondrites

Spinel group minerals always contain minor elements, such as TiO_2, V_2O_3, MnO, and ZnO (Tables 2, 3, Fig. 3). The minor element contents are indistinguishable between spinels in LL3.00–3.15 and those in LL3.2–3.3. The TiO_2 contents (in wt.%) range from 0.05 (detection limit) to 4.6 (0.86 on average) in LL3.00–3.3, 0.05–3.3 (1.30) in LL3.5–3.9, and 1.0–4.4 (2.79) in LL4–6 chondrites. The average contents increase with increasing type in LL3.00–6 chondrites. The TiO_2 contents generally decrease with increasing *mg*# (Fig. 3a). In general, there is no relationship between the occurrence of spinel and its minor element content. Even nearly pure chromites in the matrices contain 0.05–2.8% (0.73 on average) TiO_2, 0.3–1.1 (0.69) V_2O_3, 0.3–1.6 (0.47) MnO, and 0.1–0.4 (0.19) ZnO in LL3.00–3.3 chondrites.

The V_2O_3 contents range from 0.1% to 1.2% (0.48 on average) in LL3.00–3.3, 0.1–1.1 (0.69) in LL3.5–3.9, and 0.6–0.9 (0.75) in LL4–6, respectively. The average V_2O_3 contents slightly increase with type, as noted by Bunch et al. (1967). The V_2O_3 contents also decrease with increasing *mg*# (Fig. 3b). Although they show wide range of contents in LL3 chondrites, the V_2O_3 contents are homogenous in LL4–6 chondrites.

The MnO contents (in wt.%) range from 0.05 to 1.6 (0.31 on average) in LL3.00–3.3, 0.1–1.0 (0.58) in LL3.5–3.9, and 0.5–0.7 (0.62) in LL4–6 chondrites. The average

Table 3
Average and standard deviation of compositions of spinel group minerals

Sample	Class	Oca[a]	No.[b]	mg#[c]	al#	SiO_2	TiO_2	$A1_2O_3$	Cr_2O_3	V_2O_3	FeO	MnO	MgO	ZnO
Semarkona	LL3.00	All	49	0.610	0.620	0.24 ± 0.15	0.66 ± 0.54	35.31 ± 23.42	32.92 ± 21.87	0.40 ± 0.23	16.27 ± 9.77	0.36 ± 0.30	14.20 ± 8.27	b.d.
		C	43	0.650	0.640	0.23 ± 0.16	0.60 ± 0.41	40.23 ± 20.91	28.53 ± 19.92	0.34 ± 0.16	14.07 ± 8.40	0.29 ± 0.20	16.07 ± 7.13	b.d.
		M/O	6	0.050	0.000	0.29 ± 0.07	1.13 ± 1.06	0.05 ± 0.02	64.39 ± 1.68	0.84 ± 0.21	32.02 ± 1.62	0.89 ± 0.41	0.86 ± 0.97	b.d.
Y-74660	LL3.15	All	58	0.230	0.210	0.35 ± 0.19	1.02 ± 0.88	9.80 ± 15.77	55.09 ± 13.85	0.58 ± 0.26	27.13 ± 6.78	0.34 ± 0.11	4.43 ± 5.96	0.20 ± 0.21
		C	26	0.390	0.380	0.35 ± 0.20	0.89 ± 0.76	21.72 ± 17.58	44.56 ± 15.14	0.51 ± 0.32	22.10 ± 7.59	0.32 ± 0.15	9.01 ± 6.55	0.16 ± 0.31
		M/O	32	0.040	0.000	0.35 ± 0.18	1.12 ± 0.98	0.12 ± 0.13	63.65 ± 2.32	0.65 ± 0.19	31.21 ± 1.03	0.36 ± 0.07	0.71 ± 0.20	0.23 ± 0.06
Krymka	LL3.2	All	64	0.480	0.510	0.29 ± 0.17	0.50 ± 0.48	27.50 ± 28.10	40.01 ± 26.22	0.52 ± 0.26	20.92 ± 11.65	0.31 ± 0.30	10.62 ± 10.31	b.d.
		C	55	0.480	0.500	0.30 ± 0.18	0.55 ± 0.51	32.00 ± 28.10	35.52 ± 25.87	0.50 ± 0.26	19.15 ± 11.75	0.27 ± 0.27	12.30 ± 10.27	b.d.
		M/O	9	0.020	0.000	0.22 ± 0.09	0.24 ± 0.14	0.04 ± 0.01	67.42 ± 0.61	0.67 ± 0.16	31.73 ± 0.41	0.56 ± 0.35	0.33 ± 0.16	0.11 ± 0.11
Y-790448	LL3.2	All	94	0.320	0.360	0.32 ± 0.16	1.03 ± 0.97	17.80 ± 11.38	46.92 ± 9.90	0.49 ± 0.19	25.76 ± 4.97	0.32 ± 0.12	6.65 ± 4.12	0.16 ± 0.27
		C	77	0.360	0.430	0.31 ± 0.14	1.21 ± 1.72	22.18 ± 7.86	42.51 ± 6.90	0.43 ± 0.14	24.61 ± 4.89	0.29 ± 0.10	8.00 ± 3.29	0.14 ± 0.29
		M/O	17	0.040	0.010	0.34 ± 0.21	1.47 ± 0.98	0.50 ± 1.18	62.14 ± 2.84	0.73 ± 0.17	32.17 ± 0.79	0.47 ± 0.07	0.82 ± 0.34	0.30 ± 0.09
Wells	LL3.3	All	117	0.400	0.450	0.36 ± 0.45	0.65 ± 0.39	23.79 ± 8.44	44.27 ± 8.11	0.44 ± 0.11	23.10 ± 3.87	0.26 ± 0.08	8.62 ± 3.24	0.16 ± 0.19
		C	109	0.420	0.470	0.37 ± 0.47	0.62 ± 0.28	25.53 ± 5.68	42.70 ± 5.87	0.42 ± 0.07	22.47 ± 3.19	0.25 ± 0.05	9.19 ± 2.56	0.16 ± 0.20
		M/O	8	0.050	0.000	0.26 ± 0.14	1.07 ± 1.08	0.04 ± 0.01	65.72 ± 2.16	0.70 ± 0.19	31.66 ± 1.86	0.43 ± 0.14	0.85 ± 0.78	0.20 ± 0.15
ALHA77260	LL3.5	All	100	0.200	0.310	0.33 ± 0.23	1.05 ± 0.86	15.00 ± 19.42	49.24 ± 18.34	0.55 ± 0.28	28.52 ± 4.55	0.42 ± 0.15	3.96 ± 4.42	0.49 ± 0.40
		C	70	0.240	0.370	0.31 ± 0.24	0.95 ± 0.86	20.97 ± 20.62	43.50 ± 19.26	0.49 ± 0.31	27.27 ± 4.93	0.38 ± 0.17	5.23 ± 4.77	0.58 ± 0.45
		M/O	30	0.050	0.020	0.38 ± 0.19	1.30 ± 0.83	1.06 ± 1.47	62.62 ± 3.45	0.70 ± 0.10	31.44 ± 0.95	0.53 ± 0.03	0.97 ± 0.14	0.28 ± 0.04
ALHA77304	LL3.7	All	90	0.100	0.100	0.11 ± 0.11	1.35 ± 0.34	4.55 ± 3.51	59.67 ± 3.53	0.74 ± 0.07	30.16 ± 0.64	0.69 ± 0.05	1.78 ± 0.65	0.45 ± 0.06
		C	39	0.100	0.110	0.13 ± 0.10	1.28 ± 0.28	5.23 ± 5.31	59.06 ± 5.29	0.72 ± 0.10	30.01 ± 0.86	0.67 ± 0.06	1.90 ± 0.97	0.45 ± 0.06
		M/O	51	0.090	0.090	0.10 ± 0.12	1.41 ± 0.37	4.02 ± 0.29	60.13 ± 0.77	0.75 ± 0.02	30.29 ± 0.37	0.69 ± 0.04	1.68 ± 0.10	0.45 ± 0.06
BoXian	LL3.9	All	87	0.110	0.110	0.15 ± 0.12	1.60 ± 0.49	4.90 ± 5.90	58.39 ± 4.99	0.82 ± 0.14	29.85 ± 1.22	0.64 ± 0.07	1.98 ± 1.08	0.42 ± 0.08
		C	36	0.140	0.170	0.17 ± 0.14	1.56 ± 0.61	8.32 ± 8.12	55.56 ± 6.78	0.78 ± 0.19	29.39 ± 1.65	0.61 ± 0.10	2.63 ± 1.44	0.44 ± 0.10
		M/O	51	0.090	0.050	0.14 ± 0.10	1.50 ± 0.60	2.27 ± 0.57	61.57 ± 2.92	0.80 ± 0.18	30.00 ± 0.93	0.66 ± 0.04	1.59 ± 0.33	0.39 ± 0.07
Y-74002	LL4	All	190	0.090	0.130	0.07 ± 0.06	2.52 ± 0.56	5.82 ± 0.16	56.58 ± 0.86	0.76 ± 0.04	31.33 ± 0.48	0.62 ± 0.05	1.81 ± 0.18	0.39 ± 0.06
Y-74022	LL5	All	131	0.100	0.140	0.12 ± 0.11	2.63 ± 0.55	6.20 ± 0.32	55.94 ± 0.92	0.75 ± 0.03	31.17 ± 0.65	0.64 ± 0.05	1.89 ± 0.22	0.29 ± 0.06
Y-790256	LL6	All	63	0.080	0.140	0.09 ± 0.06	3.87 ± 0.48	5.91 ± 0.54	54.28 ± 0.51	0.74 ± 0.05	32.87 ± 0.38	0.59 ± 0.05	1.70 ± 0.12	0.28 ± 0.06

[a] Occurrence: All, all data; C, in chondrule; M/O, isolated grain in matrix or with opaque minerals in matrix.
[b] Number of analysis.
[c] mg#, average atomic Mg/(Mg + Fe) ratio of spinel group minerals; al#, Al/(A1 + Cr).

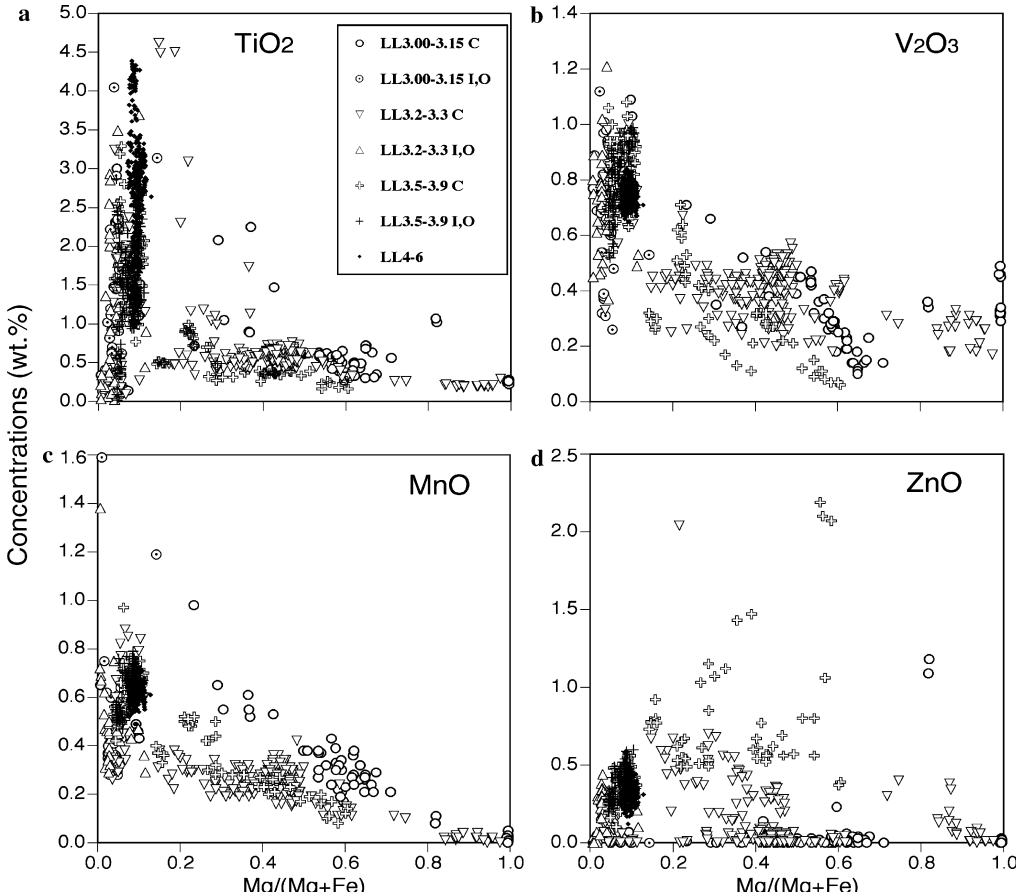

Fig. 3. Atomic Mg/(Mg + Fe) vs. minor element contents (TiO_2, V_2O_3, MnO, and ZnO) (wt.%) of spinel group minerals in LL3.00–9 chondrites.

MnO contents increase with type, and they decrease with *mg*# (Fig. 3c). The MnO contents are homogenous in the LL4–6 chondrites.

The ZnO contents (in wt.%) range from 0.1 to 2.1 (0.14 on average) in LL3.00–3.3, 0.1–2.2 (0.45) in LL3.5–3.9, and 0.1–0.6 (0.33) in LL4–6 chondrites. With increasing petrologic type, the ZnO contents increase in LL3 chondrites. Although Chikami and Miyamoto (1999) indicated that there is no correlation between type and ZnO content in LL4–6 chondrites, we find that the ZnO contents are slightly lower in the spinel from LL5–6 (~0.3%) than that in LL3.5–4 chondrites (0.4–0.5%) (Table 3). The ZnO contents seem to be independent of *mg*# in LL3–6 chondrites (Fig. 3). Yabuki et al. (1983) reported a positive correlation between the Al_2O_3 and ZnO contents in spinel in L and LL chondrites. Although Cr-spinel in LL3.5 or higher show this correlation, MgAl-spinel and Cr-spinel in LL3.00–3.3 barely contain ZnO.

3.2.3. Silicate minerals

We also measured the chemical compositions of olivine and low-Ca pyroxene in chondrules with and without spinel group minerals, and as isolated grains in the matrices. Table 4 gives the average compositions of these silicates. We were particularly interested in the Cr_2O_3 contents of the olivine, because Grossman and Brearley (2005) showed that the Cr content and variability in FeO-rich olivine is a useful indicator of metamorphic grade in very low petrologic type (3.0 to 3.2) chondrites. However, the average Cr_2O_3 contents of olivine in Semarkona and Kyrmka (Table 4) are slightly different from those reported by Grossman and Brearley (2005). This may be because the data in this study include olivine from highly magnesian chondrules, which were excluded from the classification criteria of Grossman and Brearley.

The Cr_2O_3 contents of olivine and pyroxene decrease with increasing petrologic type, e.g., 0.4% in LL3.00 to 0.07 in LL3.5 olivine. Olivine in LL3.7–6 chondrites contains essentially no Cr_2O_3, mostly below 0.03 wt% (detection limit). The decrease in Cr_2O_3 content was also observed in LL3.00–3.2 and 3.0–3.6 chondrites by Grossman and Brearley (2005) and McCoy et al. (1991b), respectively. On the other hand, the TiO_2 contents of pyroxene seem to be independent of petrologic type. Olivine contains essentially no TiO_2 (Table 4). Olivine and low-Ca pyroxene contain V_2O_3 and ZnO lower than 0.02 and 0.06 wt%, respectively.

3.3. Bulk compositions of chondrules

In order to explore the crystallization history of spinel in chondrules, we measured the bulk compositions of the

Table 4
Average compositions of olivine and low-Ca pyroxene

Sample	Class	Mineral	No.[a]	SiO_2	TiO_2	$A1_2O_3$	Cr_2O_3	FeO	MnO	MgO	CaO	Na_2O	Total
Semarkona	LL3.00	Olivine	108	41.03	b.d.	0.03	0.40	10.21	0.29	48.21	0.18	b.d.	100.35
Y-74660	LL3.15	Olivine	197	40.32	b.d.	0.02	0.24	15.13	0.31	44.21	0.15	b.d.	100.38
Krymka	LL3.2	Olivine	164	40.11	b.d.	b.d.	0.14	15.50	0.33	44.34	0.12	b.d.	100.54
Y-790448	LL3.2	Olivine	110	38.93	b.d.	0.02	0.14	20.93	0.26	39.56	0.20	b.d.	100.04
Wells	LL3.3	Olivine	140	41.16	0.03	0.09	0.10	10.24	0.20	48.84	0.28	b.d.	100.94
ALHA77260	LL3.5	Olivine	262	39.08	b.d.	0.05	0.07	21.83	0.29	38.88	0.15	b.d.	100.35
ALHA77304	LL3.7	Olivine	175	38.38	b.d.	b.d.	b.d.	23.67	0.44	37.26	b.d.	b.d.	99.75
Bo Xian	LL3.9	Olivine	86	38.12	b.d.	b.d.	0.04	25.08	0.42	36.07	b.d.	b.d.	99.73
Y-74002	LL4	Olivine	212	38.25	b.d.	b.d.	0.05	25.74	0.43	35.92	b.d.	b.d.	100.39
Y-74022	LL5	Olivine	119	38.28	b.d.	b.d.	b.d.	24.39	0.41	36.53	b.d.	b.d.	99.61
Y-790256	LL6	Olivine	98	38.01	b.d.	b.d.	b.d.	27.21	0.40	34.48	b.d.	b.d.	100.10
Semarkona	LL3.00	Low-Ca pyroxene	202	57.42	0.04	0.58	0.74	8.55	0.39	32.01	0.77	0.03	100.53
Y-74660	LL3.15	Low-Ca pyroxene	61	57.44	0.08	0.93	0.83	8.83	0.44	30.90	1.44	0.02	100.91
Krymka	LL3.2	Low-Ca pyroxene	118	58.50	0.05	0.50	0.66	5.47	0.30	34.47	0.75	0.02	100.72
Y-790448	LL3.2	Low-Ca pyroxene	26	56.91	0.06	0.66	0.66	9.49	0.36	30.76	1.20	0.04	100.14
Wells	LL3.3	Low-Ca pyroxene	76	57.96	0.11	0.85	0.75	6.65	0.34	32.95	1.21	b.d.	100.82
ALHA77260	LL3.5	Low-Ca pyroxene	44	55.78	0.14	1.85	0.67	9.72	0.33	29.61	1.83	0.08	100.01
ALHA77304	LL3.7	Low-Ca pyroxene	21	55.91	0.04	0.64	0.41	12.86	0.35	28.35	1.24	0.06	99.86
Bo Xian	LL3.9	Low-Ca pyroxene	30	56.07	0.05	0.72	0.45	11.37	0.36	28.96	1.42	0.09	99.49
Y-74002	LL4	Low-Ca pyroxene	97	55.98	0.11	0.16	0.32	15.44	0.44	27.47	0.71	b.d.	100.63
Y-74022	LL5	Low-Ca pyroxene	58	55.48	0.21	0.23	0.14	15.02	0.44	27.28	0.69	b.d.	99.49
Y-790256	LL6	Low-Ca pyroxene	30	55.39	0.15	0.13	0.06	16.20	0.40	26.54	0.92	b.d.	99.79

b.d., below detection limits (3σ,in wt%), 0.02 for $A1_2O_3$, CaO and Na_2O, 0.03 for Cr_2O_3 and TiO_2, 0.06 for MnO.
[a] Number of analysis.

chondrules that contain spinel group minerals. Table 5 shows the bulk compositions of some spinel-bearing chondrules in LL3.0–3.3 chondrites. One chondrule contains ~15 wt% Al_2O_3, which is an Al-rich chondrule based on the criteria of Bischoff and Keil (1984). All the chondrules consist of normative olivine (30–84 wt%), low-Ca pyroxene (0–53) and plagioclase (6–25) with minor amounts of high-Ca pyroxene (0–3).

Table 5 also shows *mg*# and *al*# values of spinel group minerals in these chondrules. Spinel enriched in MgO and Al_2O_3 (*mg*# >0.3 and *al*# >0.3) is encountered in Na_2O-depleted chondrules ($Na_2O < 0.6\%$), except for Wells chondrule WE-S3. Spinel enriched in FeO and Cr_2O_3 (*mg*# <0.1 and *al*# <0.3) occurs in a Na_2O-rich chondrule (Na_2O 0.8–2.1 wt%). In general, FeO-rich (type II) chondrules contain such Fe–Cr-rich spinel (Table 5), as suggested by Johnson and Prinz (1991).

3.4. Oxygen isotopic compositions of spinel group minerals

We measured the oxygen isotopic compositions of spinel group minerals and coexisting phases in chondrules from Semarkona (LL3.00) and Wells (LL3.3) (Table 6). All of the spinel group minerals measured are MgAl-spinel and Cr-spinel. Fig. 4 shows the data plotted on the three oxygen isotope diagram. All phases including euhedral to subhedral spinel in Semarkona chondrules, and olivine and two spinel grains in Wells chondrules, plot around the terrestrial fractionation (TF) line. On the other hand, an anhedral spinel in a Wells chondrule (WE-S3) (Fig. 1e) is enriched in ^{16}O ($\delta^{17}O = -5.06 \pm 1.64‰$ and $\delta^{18}O = -2.47 \pm 3.15‰$), and has significantly lighter oxygen than the coexisting olivine, which plots on the TF line (Fig. 5).

Fig. 5 shows the oxygen isotopic compositions of minerals in ferromagnesian chondrules in LL chondrites and spinels in Al-rich chondrules from unequilibrated ordinary chondrites. The oxygen isotopic compositions of all phases in Semarkona chondrules and most of the phases in Wells chondrules plot within the range of LL chondrules. However, the oxygen isotopic composition of the spinel in the Wells chondrule WE-S3 is different from compositions of LL minerals. It is also different from the highly ^{16}O-rich spinels in refractory inclusions (e.g., Hiyagon and Hashimoto, 1999) and refractory forsterite grains (Pack et al., 2004). However, the composition of the spinel in chondrule WE-S3 is within the range of spinel in Al-rich chondrules (e.g., Russell et al., 2000).

4. Discussion

4.1. Thermal metamorphism

Bunch et al. (1967) indicated that the compositions of spinel group minerals reflect petrologic types 3–6 in ordinary chondrites. Our results show that the minor as well as major element contents of the spinel are related to petrologic type in the LL3.00–3.9 chondrites. The spinel group minerals in LL3.00–3.3 chondrites can be distinguished from those in higher petrologic types (LL $\geqslant$ 3.5), by the occurrence of nearly pure chromite and MgAl-spinel, and a very wide compositional variation. In addition, the

Table 5
Bulk compositions of chondrules with spinel group minerals

Sample	Class	Chondrule	Spinel[a]	mg# Spinel[b]	al# Spinel	mg Bulk	SiO_2	TiO_2	Al_2O_3	Cr_2O_3	FeO	MnO	MgO	CaO	Na_2O	K_2O	P_2O_5	Total
Semarkona	LL3.00	S03	Cryst.	0.002	0.233	0.823	41.99	b.d.	2.21	0.70	12.98	0.34	33.97	1.23	0.91	0.12	b.d.	94.44
Semarkona	LL3.00	S04	Cryst.	0.678	0.693	0.862	38.89	0.15	1.97	0.70	11.07	0.20	38.87	1.12	0.27	b.d.	b.d.	93.23
Semarkona	LL3.00	S09	Cryst.	0.083	0.291	0.767	42.63	0.10	2.51	0.94	16.30	0.36	30.10	1.53	1.12	0.14	0.55	96.27
Semarkona	LL3.00	S10	Cryst.	0.609	0.583	0.795	42.12	0.09	2.39	1.44	14.61	0.24	31.79	1.88	b.d.	b.d.	b.d.	94.57
Y-74660	LL3.15	1	Relic	0.818	0.699	0.961	44.15	0.20	5.10	0.56	3.05	b.d.	42.54	3.45	0.14	b.d.	b.d.	99.19
Y-74660	LL3.15	2	Cryst.	0.367	0.442	0.731	47.99	0.06	2.69	0.66	17.52	0.50	26.68	1.60	0.56	b.d.	b.d.	98.26
Krymka	LL3.2	S8	Relic	0.948	0.901	0.847	39.30	0.23	15.38	0.97	9.62	b.d.	30.01	4.46	0.46	b.d.	b.d.	100.44
Wells	LL3.3	S3	Relic	0.994	0.975	0.930	43.99	0.30	5.16	0.22	5.93	b.d.	44.20	0.59	1.99	0.31	b.d.	102.69
Wells	LL3.3	S5	Cryst.	0.491	0.348	0.705	39.06	0.13	2.72	0.48	23.57	0.15	31.64	1.79	b.d.	b.d.	b.d.	99.53

b.d., below detection limits (3σ, in wt%), 0.06 for K_2O, 0.08 for TiO_2 and P_2O_5, 0.09 for Na_2O, and 0.14 for MnO.
[a] Cryst., crystallization origin in chondrule; Relic, relic origin.
[b] mg#, average atomic Mg/(Mg + Fe) ratio of spinel group minerals; al#, Al/(A1 + Cr).

apparent abundance and size of spinel group minerals are evidently different between LL3 and LL4–6 chondrites. Here we discuss the chemical variation and abundance of spinel group minerals in the context of thermal metamorphism.

Although pure MgAl-spinel and pure chromite are present in LL3.00–3.3 chondrites, the spinel group minerals, including chromite, in LL3.5–6 are not pure. The standard deviations of the major oxides, Al_2O_3, Cr_2O_3, FeO, and MgO, in spinel group minerals decrease with increasing type (Table 3). It is evident that these observations can be explained by diffusion during thermal metamorphism (e.g., Bunch et al., 1967; Johnson and Prinz, 1991). On the other hand, pure MgAl-spinel and pure chromite in LL3.00–3.3 chondrites show no evidence of chemical diffusion in the parent body, and should preserve aspects of their primordial chemical composition. Wlotzka (2005) noted that the Fe and Cr contents of spinel grains in chondrules of type 5 and 6 chondrites increase toward matrix compositions during metamorphism. Such zoning does not occur in spinel grains in type LL3.00–3.3 chondrites. Instead, they show igneous zoning.

The average *mg*# of spinel group minerals generally decreases with petrologic type (Table 3). Additionally, the range of *mg*# depends on the type: 0.01–1.00 in LL3.00–3.3, 0.04–0.61 in LL3.5, 0.05–0.29 in LL3.7–3.9, and 0.07–0.13 in LL4–6 (Fig. 2). This is explained by interdiffusion with FeO-rich phases, such as ferroan olivine in the matrix (Matsunami et al., 1990). The increase of MnO contents with petrologic type may be explained like the case of FeO. Fig. 2 and Table 3 show that the range of *mg*# is narrower than that of *al*# in LL3.5–3.9 chondrites, although both ranges are nearly the same in LL3.00–3.3. It is probable that this is due to the difference between the diffusion rates of Mg–Fe and Al–Cr. McCoy et al. (1991a) also suggested this possibility based on the diffusion patterns of spinel in L4–5 chondrites. According to the experimental work by Suzuki et al. (2005), the interdiffusion of Al–Cr is much slower than that of Mg–Fe.

The average TiO_2 contents in spinel group minerals increase from LL3 to 6, as mentioned above. On the other hand, the TiO_2 contents of low-Ca pyroxene seem to be independent of type, and the TiO_2 contents of olivine are below 0.03 wt%. Therefore, we suggest that TiO_2 diffused into the spinel group minerals from other phases, such as the groundmass glass in chondrules and/or high-Ca pyroxene. Rubin (1986) showed that chondrule glasses contain 2.5–3.0 wt% TiO_2. On the other hand, high-Ca pyroxene in LL3.0–3.4 contains 0.1–2.9 wt% (0.53% in average) TiO_2 (Noguchi, 1989), whereas that in LL4–6 contains 0.2-0.4 wt% (0.38) (Heyse, 1978). The lower values of TiO_2 of high-Ca pyroxene in LL4–6 chondrites may be related to the increase in TiO_2 in the spinel group minerals in the higher petrologic types.

The V_2O_3 contents also increase with type. Although the V_2O_3 contents of olivine and pyroxene are lower than 0.02 wt%, Allen and Mason (1973) showed that olivine

Table 6
Oxygen isotopic compositions of silicates and MgAl-spinels in chondrules of Semarkona and Wells

Position	Phase[a]	mg# of ol, lpx, sp[b]	$\delta^{17}O$ (‰)[c]	$\delta^{18}O$(‰)[c]	$\Delta^{17}O$ (‰)[c,d]
Semarkona					
10B	sp	0.585	4.04 ± 1.91	6.84 ± 1.67	0.48 ± 1.88
10C	lpx	0.795	2.98 ± 2.03	4.52 ± 1.81	0.63 ± 2.04
11A	ol	0.995	1.50 ± 2.08	1.46 ± 1.93	0.74 ± 2.11
11D	hpx, pl		0.45 ± 2.06	1.57 ± 1.89	−0.36 ± 2.09
11-5	ol, hpx, pl	0.995	2.36 ± 1.64	2.34 ± 2.41	1.15 ± 2.01
11-2b	sp	0.995	−1.30 ± 1.67	−0.30 ± 2.34	−1.14 ± 2.01
11-3b	ol	0.995	0.60 ± 1.68	4.62 ± 2.32	−1.80 ± 2.01
11-4b	hpx, pl		4.43 ± 1.45	6.99 ± 2.44	0.79 ± 1.87
4E	ol	0.881	4.10 ± 1.69	7.77 ± 2.51	0.06 ± 1.55
4F2	sp	0.705	5.51 ± 2.00	10.35 ± 2.51	0.13 ± 1.89
Wells					
S1-01	ol	0.876	6.65 ± 2.54	12.47 ± 3.39	0.16 ± 2.07
S1-02	ol	0.876	5.43 ± 2.38	11.43 ± 3.27	−0.52 ± 1.82
S3-01	ol	0.991	0.23 ± 1.79	1.54 ± 3.21	−0.57 ± 1.99
S3-02	sp	0.975	−5.06 ± 1.64	−2.47 ± 3.15	−3.78 ± 1.83
S5-01	ol	0.751	6.39 ± 1.73	8.30 ± 3.23	2.07 ± 1.94
S5-03	ol	0.751	3.31 ± 1.50	8.51 ± 3.14	−1.11 ± 1.70
S5-02b	sp	0.348	6.88 ± 1.65	12.22 ± 3.11	0.53 ± 1.82
S6-01	ol	0.771	6.45 ± 1.64	7.13 ± 3.16	2.74 ± 1.83
S6-02	sp	0.443	7.62 ± 1.50	9.32 ± 3.15	2.77 ± 1.70

[a] Analysis phases: sp, spinel group minerals; lpx, low-Ca pyroxene; ol, olivine; hpx, high-Ca pyroxene; pl, plagioclase.
[b] atomic Mg/(Mg + Fe) ratio.
[c] Errors 1σ.
[d] $\Delta^{17}O = \delta^{17}O - 0.52 \times \delta^{18}O$ (‰).

and low-Ca pyroxene in L6 chondrites contain 9 and 40 ppm V, respectively. Since the abundance of olivine and pyroxene is much higher than that of spinel group minerals, the increase in V_2O_3 contents with type might be explained by diffusion of V from the silicates to spinel group minerals during thermal metamorphism.

The ZnO contents of spinel group minerals show a positive correlation with petrologic type, as suggested by Johnson and Prinz (1991). Zinc might have been primarily contained in troilite, and was later redistributed into chromite (Johnson and Prinz, 1991). On the other hand, olivine and low-Ca pyroxene in L6 chondrites contain 20 and 17 ppm Zn, respectively (Allen and Mason, 1973). Klöck et al. (1999) suggested that ~50% of bulk Zn is present in silicates in type 3 ordinary chondrites. We can not exclude the possibility that part of the Zn was primarily included in the silicates in type 3 chondrites, and later diffused into spinel.

The abundance and size of spinel group minerals are smaller in LL3 than those in LL4–6 chondrites (Table 1). On the other hand, the average Cr_2O_3 contents of olivine and low-Ca pyroxene decrease with increasing type (Table 4). This may be related to the formation of chromite during thermal metamorphism. From the modal data by Gastineau-Lyons et al. (2002), olivine and low-Ca pyroxene occupy ~50 and ~20 wt% of LL4–6 chondrites, respectively. From these modal data and Cr_2O_3 contents of olivine and low-Ca pyroxene, we estimated that ~0.5 wt% chromite can form from the release of Cr from olivine and low-Ca pyroxene. This is consistent with the increase in the abundance of spinel group minerals in LL3–6 chondrites studied here. The average *al*# of spinel group minerals decreases with petrologic type. This can be explained by such secondary formation of chromite.

Grossman and Brearley (2005) found that a Cr-rich phase, <1 μm in size, exsolved from olivine in an L3.10 chondrite. This may be chromite. It is probable that chromite increases in size with petrologic type (or degree of metamorphism), and can be recognized as coarse grains in chondrites of higher types, as observed in this study.

Here, we conclude that the characteristic features of spinel group minerals should be a good indicator of petrologic type and thermal metamorphism in LL chondrites. We predict that spinel will also be a good indicator of thermal metamorphism in the other chondrite groups. However, the characteristic features of spinel group minerals remain unchanged from type 3.00 to 3.3, as mentioned above. Therefore, the chemical compositions and size distribution of spinel group minerals alone can not be used to distinguish between the lowest petrologic types.

4.2. Geothermometry

Although many olivine–spinel geothermometers have been proposed, Weinbruch et al. (1994) compared them and found that the method of Roeder et al. (1979) gives the most realistic temperatures for Allende. Fig. 6 shows olivine–spinel geothermometry after the method of Roeder et al. (1979). We used olivine–spinel data from chondrules in LL3 and from chondrules and matrices in LL4–6 chon-

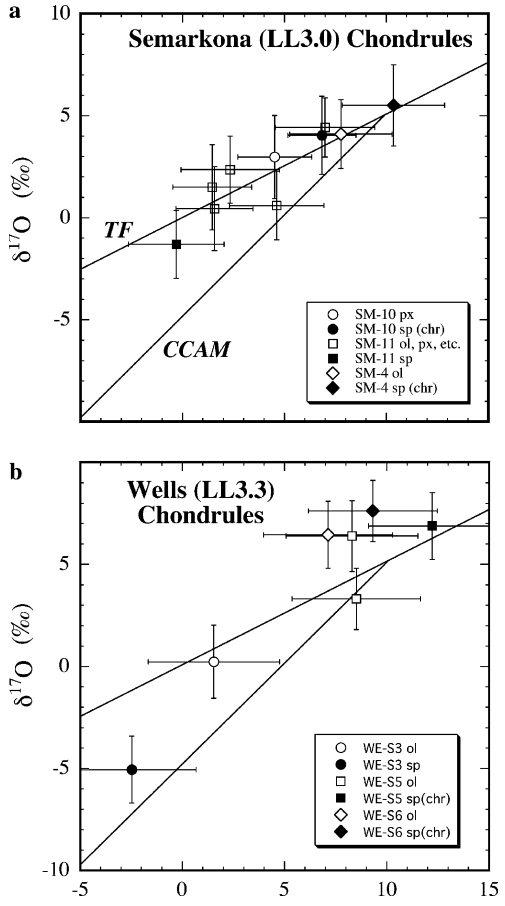

Fig. 4. Oxygen isotopic compositions of spinel group minerals and coexisting phases in (a) Semarkona (LL3.00) and (b) Wells (LL3.3). Note that spinel in a chondrule (S3) in Wells is enriched in ^{16}O, and has significantly lighter oxygen than the coexisting olivine, which plots on the terrestrial fractionation (TF) line. CCAM, carbonaceous chondrite anhydrous mixing line. ol, olivine; px, pyroxene; sp, spinel. Error bars are 1σ.

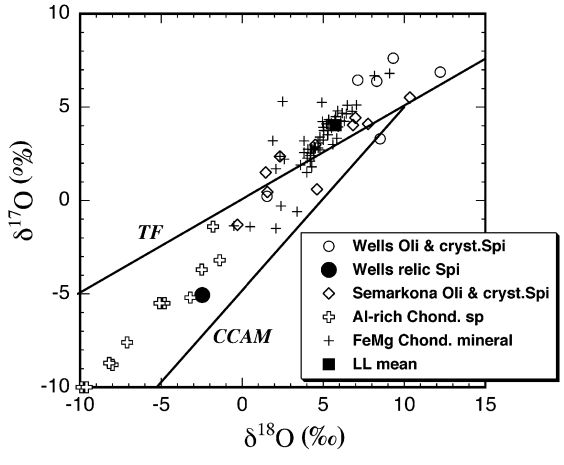

Fig. 5. Oxygen isotopic compositions of spinel and silicates in chondrules of Semarkona and Wells, compared with those in ferromagnesian chondrules and Al-rich chondrules, and mean composition of LL chondrites, after Bridges et al. (1998, 1999); Li et al. (2000); Sears et al. (1998); Russell et al. (2000) and Clayton et al. (1991). It is noted that a Wells spinel has a composition within the range of spinel in Al-rich chondrules.

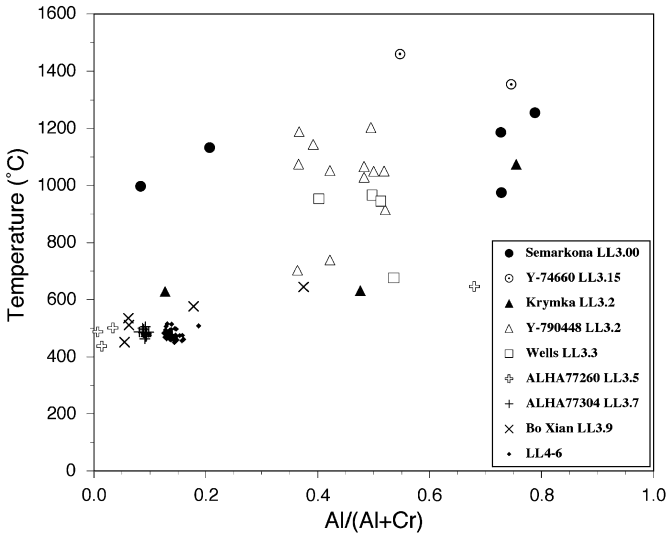

Fig. 6. Spinel–olivine geothermometry on atomic Al/(Al + Cr) of spinel group minerals vs. temperature (°C) after the method by Roeder et al. (1979). Note that most of the olivine–spinel pairs in LL3.00–3.3 give high temperatures reflecting crystallization in the chondrule. On the other hand, the pairs in LL3.5–6 show metamorphic temperatures of 440–650 °C.

drites. We did not use olivine–spinel pairs from the matrix of LL3 chondrites because it is difficult to determine if they are in equilibrium.

Most of the olivine–spinel pairs in LL3.00–3.3 give high (above 1000 °C) temperatures, which is consistent with the results of Johnson and Prinz (1991). These high temperatures most likely reflect the conditions of chondrule crystallization. On the other hand, the pairs in LL3.5–6 show temperatures of 440–650 °C, in spite of the *al*# of the spinel and its occurrence. Such low temperatures should reflect the closure temperatures after thermal metamorphism (Wlotzka, 2005). FeO and MgO thoroughly diffused between olivine and spinel group minerals in type $\geqslant$3.5 chondrites during thermal metamorphism. This is consistent with the narrow to homogeneous compositional distribution of spinel group minerals in these chondrites. The metamorphic temperatures for LL3.00–3.3 chondrites were lower than those for type $\geqslant$3.5, and/or the duration of metamorphism was much shorter than those for type $\geqslant$3.5 chondrites. Thus, the olivine–spinel pairs in LL3.00–3.3 chondrites preserved their primary crystallization temperatures. Low metamorphic temperatures for these chondrites are also supported by the presence of hydrous phases (Alexander et al., 1989), and the compositions of sulfide (Quirico et al., 2003) and Fe–Ni metal (Kimura et al., 2005).

Recently, Kimura et al. (2005) showed that the characteristic features of Fe–Ni metal, such as chemical composition and texture, systematically change from type 3.00 to 3.2, which is different from spinel group minerals. The difference between spinel group minerals and Fe–Ni metal in types 3.00–3.3 may reflect differences in their diffusion rates; the diffusion rate for metal is much higher than that

for spinel (Dean and Goldstein, 1986; Liermann and Ganguly, 2002).

4.3. Crystallization of spinel in chondrules

Here, we discuss the origin and crystallization of spinel group minerals within chondrules in type 3 chondrites. Spinel in the groundmass or among chondrule phenocrysts is euhedral to subhedral in form (Fig. 1c and d), indicating that it crystallized from the chondrule melt. Fig. 7 shows the bulk compositions of several chondrules on the forsterite–anorthite–silica phase diagram. We use this diagram because these chondrules mostly consist of normative olivine, low-Ca pyroxene and anorthitic plagioclase as mentioned before. The Na_2O-rich chondrules (>0.6%) are more enriched in normative albite than anorthite, and the bulk compositions of these chondrules are not plotted on this diagram.

Fig. 7 shows that the crystallization sequence of the chondrules analyzed here is olivine, through low-Ca pyroxene in some cases, to anorthitic plagioclase. We would not expect crystallization of spinel in these chondrules. Only in a few cases, we may expect crystallization of spinel after olivine. Although the incorporation of FeO affects the phase boundaries of the forsterite–anorthite–silica system (Longhi and Pan, 1988), the bulk FeO contents of these chondrules are not very high (*mg*# of 0.71–0.96). The crystallization sequence should remain essentially unchanged from the FeO-free system for these chondrules. The incorporation of Na_2O reduces the liquidus field of plagioclase in the forsterite–anorthite–silica system (Sessler et al., 1982; Longhi and Pan, 1988). However, the crystallization sequence for the chondrule bulk compositions also remains unchanged.

On the other hand, Onuma (1984) showed that incorporation of Cr_2O_3 significantly expands the liquidus field of spinel in the forsterite–anorthite–silica system (Fig. 7), and we expect extensive crystallization of spinel in various bulk compositions with small Cr_2O_3 contents. Fig. 7 shows that the crystallization sequences of the chondrules is olivine, through low-Ca pyroxene, to spinel, or olivine followed directly by spinel. This sequence is consistent with the occurrence of euhedral to subhedral Cr-spinel in the chondrules (Table 5), which is associated with olivine and pyroxene phenocrysts, and within the groundmass glass (Figs. 1c and d). Igneous zoning as mentioned before also supports crystallization of the spinel from the chondrule melts. Indeed, the Cr_2O_3 contents of these chondrules are 0.2–1.4 wt%, which is generally consistent with the experimental work by Onuma (1984).

4.4. Relic origin of spinel in chondrules

Some spinel grains, 5–35 μm in size, are completely enclosed within single olivine phenocrysts in several chondrules. These grains usually show spherical to irregular forms (Fig. 1e), and are MgAl-spinel or Cr-spinel (Tables 2 and 5). From their occurrence, the crystallization sequence must be from spinel, through olivine, to groundmass glass (plagioclase). Although these chondrules also contain 0.2–1.0 wt% Cr_2O_3, the bulk compositions of the chondrules indicate that olivine should have crystallized

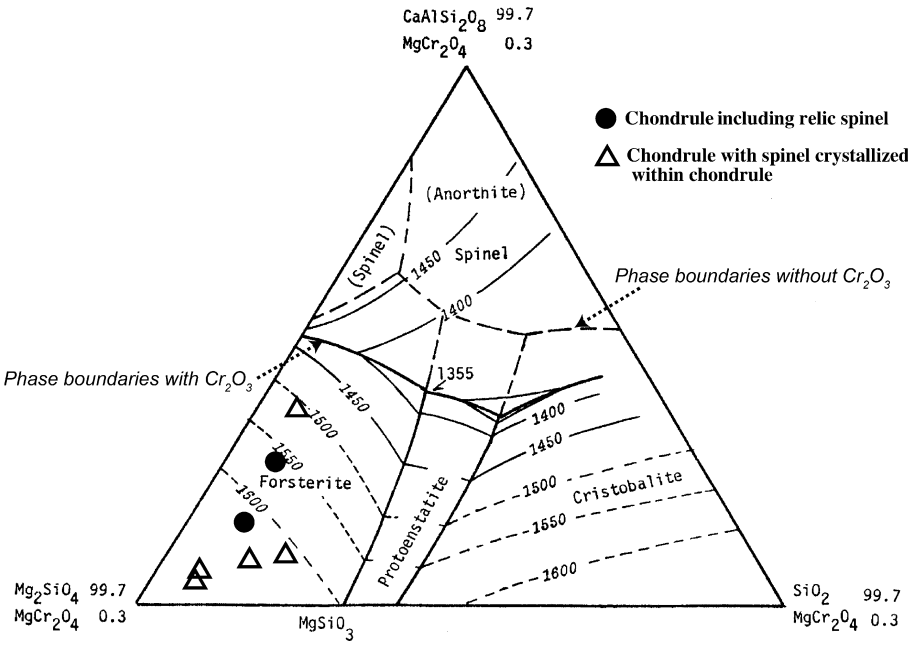

Fig. 7. Plot of bulk compositions of chondrules on the anorthite–forsterite–silica diagram, after Levin et al. (1964). Chondrules including relic spinel are shown by filled circle, and the open triangles show chondrules with spinel that crystallized within the chondrule. The phase boundaries with the addition of Cr_2O_3 are shown by dashed lines, after Onuma (1984). It is noted that the spinel liquidus field significantly expands by the incorporation of Cr_2O_3, in comparison with the field free from Cr_2O_3 denoted by (spinel).

first even in Cr_2O_3-bearing systems (Fig. 7). The occurrence of the spinel grains included in olivine is, therefore, inconsistent with the crystallization of the chondrules from these bulk compositions.

Although Grossman and Brearley (2005) noted a Cr-rich phase exsolved from olivine in a L3.10 chondrite, it is smaller than 1 μm in size, which is much smaller than the spinels described above. Additionally, these spinels within olivine phenocrysts are not chromite, but highly enriched in Al_2O_3 (Tables 2 and 5). Olivine does not contain Al_2O_3, and these MgAl-spinel and Cr-spinel minerals are evidently different from the exsolved phase in olivine reported by Grossman and Brearley.

Therefore, we suggest that these spinel grains are not crystallization products of the chondrule, but are relic grains. They were incorporated into the chondrule precursor materials before melting. Because of high melting temperatures, some spinel grains survived melting of the chondrule precursor material. We found such relic spinel grains in Y-74660 (LL3.15), Krymka (LL3.2) and Wells (LL3.3). We determined that they are relic grains based on their textural settings and the bulk compositions of their host chondrules (Table 5). However, we note that the relic spinel is not compositionally distinct from some of the spinel grains that apparently crystallized in the chondrules (Table 2).

The relic origin of some MgAl-spinel and Cr-spinel in chondrules is clearly supported by oxygen isotope data. A relic spinel in a magnesian chondrule from Wells that we analyzed for oxygen is enriched in ^{16}O and plots below the TF line. It is clearly different from the surrounding ^{16}O-poor olivine in the same chondrule (Fig. 4b). This spinel could not have crystallized together with the olivine from the chondrule melt. On the other hand, silicates and euhedral to subhedral spinels in the groundmasses of three Semarkona and two Wells chondrules, plot around the TF line (Fig. 4). This is consistent with the phase equilibria discussed above that indicates they crystallized from the chondrule melt.

Diffusion of oxygen in spinel is very slow. Even at 1400 °C, the diffusion of oxygen for a 1 μm distance takes ~1300 h, from the data of Ryerson and McKeegan (1994). Therefore, it is difficult for the oxygen isotopic composition of the relic spinel to completely equilibrate with that of the surrounding olivine, during chondrule formation by flash heating (e.g., Lofgren, 1996). Thus, it is likely that the oxygen of the relic spinel did not equilibrate with the chondrule melt and it still preserves its primordial oxygen isotopic composition.

The oxygen composition of the MgAl-spinel in the Wells chondrule is different from the highly ^{16}O-rich spinels in refractory inclusions and the spinels in refractory forsterite in ordinary chondrites. Although spinel is the most common mineral in refractory inclusions in ordinary chondrites (e.g., Kimura et al., 2002; Lin et al., 2006), the relic spinel is not genetically related to refractory inclusions. The oxygen isotopic composition of the relic spinel is most similar to that of spinel in Al-rich chondrules (Fig. 5). Al-rich chondrules have characteristics that are intermediate between refractory inclusions and ferromagnesian chondrules (e.g., MacPherson and Huss, 2005). It is probable that the relic spinel may have been derived from an Al-rich chondrule.

Relic components have been reported from carbonaceous chondrites, such as fragments of refractory inclusions in ferromagnesian chondrules (Misawa and Fujita, 1994) and in Al-rich chondrules (Krot et al., 2002), ^{16}O-enriched relic spinel in chondrules (Maruyama et al., 1999), and relic olivine in chondrules (Jones et al., 2004). However, relic components are less commonly observed in ordinary chondrites, such as relict grains of magnesian silicates in FeO-rich chondrules (Jones, 1990) and relic perovskite in a ferromagnesian chondrule (Kimura et al., 2004). We predict that relic components are more common in ordinary chondrites than previously reported. However, further work is needed to test this hypothesis.

Our discovery of a relic spinel in a chondrule is an indication of the complexities in the early solar nebula processes that ranged from formation of refractory inclusions, through Al-rich chondrules, to ferromagnesian chondrules. Some of the earlier-formed minerals like spinel may have been incorporated as part of the mixture of precursors that formed subsequent components and some survived melting.

4.5. Origin of chromite in the matrix

Nearly pure chromites are present in the matrix, often associated with Fe–Ni metal and troilite, in LL3.00–3.3 chondrites. We consider four mechanisms for the origin of these chromites: (1) fragments from chondrules, (2) secondary metamorphic reaction between silicate and/or oxide minerals, (3) oxidation from Fe–Ni metal, and (4) direct condensation.

Especially in primitive chondrites of type 3.00–3.3, the chromite composition is completely different from that of MgAl-spinel and Cr-spinel in chondrules. The occurrence is inconsistent with exsolution from Cr-bearing silicate phases, and secondary reaction between matrix phases. The pure chromite does not show any reaction textures with the surrounding silicate and/or oxide minerals. Therefore, we can exclude the possibility of its origin through (1) fragmentation of chondrules and (2) metamorphic reaction in the parent body.

Some Fe–Ni metal in type 3 chondrites contains detectable Cr (e.g., Zanda et al., 1994; Kimura, 2000). Condensation of Cr dissolved in Fe–Ni metal is expected (e.g., Grossman and Olsen, 1974). Zanda et al. (1994) showed the inclusion of secondary chromite within Fe–Ni metal in some carbonaceous chondrites. Lauretta et al. (2001) found tiny chromite grains on the rim of Fe–Ni metal in Bishunpur (LL3.15). Such chromite formed by oxidation of Cr dissolved in Fe–Ni metal. Thus, a possible origin for the pure chromites is oxidation of Cr-bearing Fe–Ni metal. However, the pristine chromites found in this study

always contain some TiO_2, V_2O_3, MnO, and ZnO, as mentioned above, which can not be simply explained by the oxidation of metal. These elements are not expected to condense into Fe–Ni metal. The diffusion of TiO_2 and other minor elements from the surrounding matrix is excluded, unless their diffusion rates are much higher than those of Al_2O_3 and MgO. The isolated occurrence of pure chromite in the matrix without associated Fe–Ni metal seems to be inconsistent with an oxidation origin, unless the chromite is a fragment from Fe to Ni metal.

An alternative explanation is that the chromite condensed directly from the nebula under high temperatures, more than ~1400 K, depending on the oxygen fugacity (e.g., Palme and Fegley, 1990; Krot et al., 1993). These chromites might have formed through condensation onto surfaces of metal grains. However, chromite that condensed from the nebular gas under equilibrium conditions is expected to contain MgO and Al_2O_3 (Ebel and Grossman, 2000; Petaev, personal communication, 2006). It has not yet been calculated whether such chromite condensates can contain TiO_2 and V_2O_3. Further study, including condensation calculations, is needed to better understand the origin of these chromites.

5. Conclusions

We reported the results of our systematic study of spinel group minerals in LL3.00–6 chondrites. The chemical compositions, size distribution and abundance of spinel group minerals are related to petrologic type 3.00–6. The occurrence of nearly pure chromite and MgAl-spinel, and the wide compositional variation distinguish spinel group minerals in type 3.00–3.3 from those in the higher petrologic types. Metamorphic effects can explain the increase in abundance and compositional changes of spinel group minerals that we observed. Thus, the characteristic features of spinel are a good indicator of petrologic type and metamorphic conditions not only for equilibrated chondrites, but also for type 3 chondrites. Spinel group minerals are a more sensitive indicator for thermal metamorphism of chondrites of low types, in comparison with some silicates. They can also be applied to help identify the most primitive (least metamorphosed) chondrites.

Most of the spinel group minerals in chondrules crystallized from the chondrule melt. However, some spinel grains enclosed in olivine phenocrysts may be relic grains, as indicated by their oxygen isotopic compositions and phase relations. Thus, they preserve a nebular history that predates chondrule formation. The occurrence of such grains indicates the complexities in the early solar nebula processes ranging from formation of refractory inclusions, through Al-rich chondrules, to ferromagnesian chondrules, and the recycling of earlier formed materials into the precursor mixture of later formed ones.

Acknowledgments

We thank H. Kojima of the National Institute of Polar Research in Japan, D. Ebel and J. Bosenberg of the American Museum of Natural History, and Y. Lin of Chinese Academy of Science for sample allocation. We are grateful to D. Ebel for discussions. We appreciate the thorough reviews by M.I. Petaev and an anonymous reviewer. The comments of the associate editor, A.N. Krot, were helpful in revising the manuscript. This study was supported by the Grant-in-Aid for Scientific Research from the Ministry of Education, Science and Culture of Japan, No. 16540435 (M. Kimura) and NASA Grant NAG5-11546 (M. Weisberg, P.I.).

Associate editor: Alexander N. Krot

References

Alexander, C.M.O., Barber, D.J., Hutchison, R., 1989. The microstructure of Semarkona and Bishunpur. *Geochim. Cosmochim. Acta* **53**, 3045–3057.

Allen, R.O., Mason, B., 1973. Minor and trace elements in some meteoritic minerals. *Geochim. Cosmochim. Acta* **37**, 1435–1456.

Bischoff, A., Keil, K., 1984. Al-rich objects in ordinary chondrites: related origin of carbonaceous and ordinary chondrites and their constituents. *Geochim. Cosmochim. Acta* **48**, 693–709.

Brearley, A.J., Jones, R.H., 1998. Chondritic meteorites. In: Papike, J.J. (Ed.), *Planetary Materials*, Vol. 36. Mineralogical Soc., America, Washington DC, pp. 1–398.

Bridges, J.C., Franchi, I.A., Hutchison, R., Sexton, A.S., Pillinger, C.T., 1998. Correlated mineralogy, chemical compositions, oxygen isotopic compositions and size of chondrules. *Earth Planet. Sci. Lett.* **155**, 183–196.

Bridges, J.C., Franchi, I.A., Sexton, A.S., Pillinger, C.T., 1999. Mineralogical controls on the oxygen isotopic compositions of UOCs. *Geochim. Cosmochim. Acta* **63**, 945–951.

Bridges, J.C., Schmitz, B., Hutchison, R., 2004. Petrographic classification and chondrule textures of fossil meteorites from southern Sweden (abstract). *Meteorit. Planet. Sci.* **39** (Suppl.), A17.

Bunch, T.E., Keil, K., Snetsinger, K.G., 1967. Chromite composition in relation to chemistry and texture of ordinary chondrites. *Geochim. Cosmochim. Acta* **31**, 1569–1582.

Chikami, J., Miyamoto, M., 1999. Zn content of chromites in different petrologic type LL chondrites (abstract). *Lunar Planet. Sci.* **XXX**, 1167, Lunar and Planet. Inst., Houston.

Clayton, R.N., Mayeda, T.K., Goswami, J.N., Olsen, E.J., 1991. Oxygen isotope studies of ordinary chondrites. *Geochim. Cosmochim. Acta* **55**, 2317–2337.

Dean, D.C., Goldstein, J.I., 1986. Determination of the interdiffusion coefficients in the Fe–Ni and Fe–Ni–P systems below 900 °C. *Meteorit. Trans.* **17A**, 1131–1138.

Deer, W.A., Howie, R.A., Zussman, J., 1992. *An Introduction to the Rock-Forming Minerals*. Longman, Hong Kong, 696p.

Ebel, D.S., Grossman, L., 2000. Condensation in dust-enriched systems. *Geochim. Cosmochim. Acta* **64**, 339–366.

Gastineau-Lyons, H.K., McSween Jr., H.Y., Gaffey, M.J., 2002. A critical evaluation of oxidation versus reduction during metamorphism of L and LL group chondrites, and implications for asteroid spectroscopy. *Meteorit. Planet. Sci.* **37**, 75–89.

Grossman, L., Olsen, E., 1974. Origin of the high-temperature fraction of C2 chondrites. *Geochim. Cosmochim. Acta* **38**, 173–187.

Grossman, J.N., Brearley, A.J., 2005. The onset of metamorphism in ordinary and carbonaceous chondrites. *Meteorit. Planet. Sci.* **40**, 87–122.

Heyse, J.V., 1978. The metamorphic history of LL-group ordinary chondrites. *Earth Planet. Sci. Lett.* **40**, 365–381.

Hiyagon, H., Hashimoto, A., 1999. ^{16}O excesses in olivine inclusions in Yamato-86009 and Murchison chondrites and their relation to CAI. *Science* **283**, 828–831.

Ikeda, Y., 1980. Petrology of Allan Hills-764 chondrite (LL3). *Mem. Natl. Inst. Polar Res. Spec. Issue* **17**, 50–82.

Johnson, C.A., Prinz, M., 1991. Chromite and olivine in type II chondrules in carbonaceous and ordinary chondrites: implications for thermal histories and group differences. *Geochim. Cosmochim. Acta* **55**, 893–904.

Jones, R.H., 1990. Petrology and mineralogy of type II, FeO-rich chondrules in Semarkona (LL 3.0): origin by closed-system fractional crystallization, with evidence for supercooling. *Geochim. Cosmochim. Acta* **54**, 1785–1802.

Jones, R.H., Leshin, L.A., Guan, Y., Sharp, Z.D., Durakiewicz, T., Schilk, A.J., 2004. Oxygen isotope heterogeneity in chondrules from the Mokoia CV3 carbonaceous chondrite. *Geochim. Cosmochim. Acta* **68**, 3423–3438.

Keil, K., 1962. On the phase composition of meteorites. *J. Geophys. Res.* **67**, 4055–4061.

Kimura, M., 2000. Opaque minerals in an LL3.0 chondrite, Y74660: potential indicators of petrologic subtypes (abstract). *Lunar Planet. Sci.* **23**, 1213, Lunar and Planet. Inst., Houston.

Kimura, M., Hiyagon, H., Palme, H., Spettel, B., Wolf, D., Clayton, R.N., Mayeda, T.K., Sato, T., Suzuki, A., Kojima, H., 2002. The most primitive H-chondrites: Y792947, Y793408 and Y82038, with abundant refractory inclusions. *Meteorit. Planet. Sci.* **37**, 1417–1434.

Kimura, M., Nakajima, H., Weisberg, M.K., 2003. Spinel, Ti-oxides and Fe–Ni metal in LL3.0–6 chondrites: indicators of primordial and secondary processes (abstract). *Meteorit. Planet. Sci.* **38** (Suppl.), A33.

Kimura, M., Sugiura, N., Nakajima, H., Weisberg, M.K., 2004. Opaque minerals in LL3.0–6 chondrites I: Mineralogy of Ti-oxides and ^{53}Mn–^{53}Cr systematics of ilmenite. *Acta Geol. Sin.* **78**, 1082–1089.

Kimura, M., Grossman, J.N., Weisberg, M.K., Nakajima, H., 2005. Fe–Ni metal and spinel group minerals in LL3 chondrites: metamorphic conditions of highly primitive chondrites (abstract). *Antarct. Meteorite* **XXIX**, 28–29.

Kita, N.T., Nagahara, H., Togashi, S., Morishita, Y., 2000. A short duration of chondrule formation in the solar nebula: evidence from ^{26}Al in Semarkona ferromagnesian chondrules. *Geochim. Cosmochim. Acta* **64**, 3913–3922.

Klöck, W., Maetz, M., Nakamura, K., Wies, C., 1999. Zinc contents of chondrite silicates of different petrologic types (abstract). *Meteorit. Planet. Sci.* **34** (Suppl.), A65–A66.

Krot, A.N., Ibanova, M.A., Wasson, J.T., 1993. The origin of chromitic chondrules and the volatility of Cr under a range of nebular conditions. *Earth Planet. Sci. Lett.* **119**, 569–584.

Krot, A.N., Hutcheon, I.D., Keil, K., 2002. Plagioclase-rich chondrules in the reduced CV chondrites: evidence for complex formation history and genetic links between CAIs and ferromagnesian chondrules. *Meteorit. Planet. Sci.* **37**, 155–182.

Lauretta, D.S., Buseck, P.B., Zega, T.J., 2001. Opaque minerals in the matrix of the Bishunpur (LL3.1) chondrite: constraints on the chondrule formation environment. *Geochim. Cosmochim. Acta* **65**, 1337–1353.

Levin, E.M., Robbins, C.R., McMurdie, H.F., 1964. *Phase Diagrams for Ceramists*. The American Ceramic Society, Ohio, 601p.

Li, C., Bridges, J.C., Hutchison, R., Franchi, I.A., Sexton, A.S., Ouyang, Z., Pillinger, C.T., 2000. Bo Xian (LL3.9): oxygen-isotopic and mineralogical characterisation of separated chondrules. *Meteorit. Planet. Sci.* **35**, 561–568.

Liermann, H.-P., Ganguly, J., 2002. Diffusion kinetics of Fe^{2+} and Mg in aluminous spinel: experimental determination and applications. *Geochim. Cosmochim. Acta* **66**, 2903–2913.

Lin, Y., Kimura, M., Miao, B., Dai, D., Monoi, A., 2006. Petrographic comparison of refractory inclusions from different chemical groups of chondrites. *Meteorit. Planet. Sci.* **41**, 67–81.

Lofgren, G.E., 1996. A dynamic crystallization model for chondrule melts. In: Hewins, R.H., Jones, R.H., Scott, E.R.D. (Eds.), *Chondrules and the Protoplanetary Disk*. Cambridge University Press, Cambridge, pp. 187–196.

Longhi, J., Pan, V., 1988. A Reconnaissance study of phase boundaries in low-alkali basaltic liquids. *J. Petrol.* **29**, 115–147.

MacPherson, G.J., Huss, G.R., 2005. Petrogenesis of Al-rich chondrules: evidence from bulk compositions and phase equilibria. *Geochim. Cosmochim. Acta* **69**, 3099–3127.

Maruyama, S., Yurimoto, H., Sueno, S., 1999. Oxygen isotope evidence regarding the formation of spinel-bearing chondrules. *Earth Planet. Sci. Lett.* **169**, 165–171.

Matsunami, S., Nishimura, H., Takeshi, H., 1990. The chemical compositions and textures of matrices and chondrule rims of unequilibrated ordinary chondrites –II. Their constituents and the implications for the formation of matrix olivine. *Proc. NIPR Symp. Antarct. Meteorites* **3**, 147–180.

McCoy, T.J., Pun, A., Keil, K., 1991a. Spinel-bearing, Al-rich chondrules in two chondrite finds from Roosevelt County, New Mexico: indicators of nebular and parent body processes. *Meteoritics* **26**, 301–309.

McCoy, T.J., Scott, E.R.D., Jones, R.H., Keil, K., Taylor, G.J., 1991b. Composition of chondrule silicates in LL3-5 chondrites and implications for their nebular history and parent body metamorphism. *Geochim. Cosmochim. Acta* **55**, 601–619.

Misawa, K., Fujita, T., 1994. A relict refractory inclusion in a ferromagnesian chondrule from the Allende meteorite. *Nature* **368**, 723–726.

Nehru, C.E., Weisberg, M.K., Prinz, M., 1997. Chromites in unequilibrated ordinary chondrites (abstract). *Lunar Planet. Sci.* **XXVIII**, 1651, Lunar and Planet. Inst., Houston.

Noguchi, T., 1989. Texture and chemical composition of pyroxenes in chondrules in carbonaceous and unequilibrated ordinary chondrites. *Proc. NIPR Symp. Antarct. Meteorites* **2**, 168–199.

Onuma, K., 1984. Liquidus phase relations on the join forsterite–anorthite–silica with 0.3% $MgCr_2O_4$ in air at 1 atm. *J. Jan. Assoc. Min. Petr. Econ. Geol.* **79**, 387–393.

Pack, A., Yurimoto, H., Palme, H., 2004. Petrographic and oxygen-isotopic study of refractory forsterites from R-chondrite Dar al Gani 013 (R3.5–6), unequilibrated ordinary and carbonaceous chondrites. *Geochim. Cosmochim. Acta* **68**, 1135–1157.

Palme, H., Fegley, B., 1990. High-temperature condensation of iron-rich olivine in the solar nebula. *Earth Planet. Sci. Lett.* **101**, 180–195.

Quirico, E., Raynal, P.-I., Bourot-Denise, M., 2003. Metamorphic grade of organic matter in six unequilibrated ordinary chondrites. *Meteorit. Planet. Sci.* **38**, 795–811.

Roeder, P.L., Campbell, I.H., Jamieson, H.E., 1979. A re-evaluation of the olivine–spinel geothermometer. *Contrib. Mineral. Petrol.* **68**, 325–334.

Rubin, A.E., 1986. Elemental compositions of major silicate phases in chondrules of unequilibrated chondritic meteorites. *Meteoritics* **21**, 283–293.

Rubin, A.E., 2003. Chromite-plagioclase assemblages as a new shock indicator; implications for the shock and thermal histories of ordinary chondrites. *Geochim. Cosmochim. Acta* **67**, 2695–2709.

Russell, S.S., MacPherson, G.J., Leshin, L.A., McKeegan, K.D., 2000. ^{16}O enrichments in aluminum-rich chondrules from ordinary chondrites. *Earth Planet. Sci. Lett.* **184**, 57–74.

Ryerson, F.J., McKeegan, K.D., 1994. Determination of oxygen self-diffusion in åkermanite, anorthite, diopside, and spinel: implications for oxygen isotopic anomalies and the thermal histories of Ca–Al-rich inclusions. *Geochim. Cosmochim. Acta* **58**, 3713–3734.

Sears, D.W.G., Dodd, R.T., 1988. Overview and classification of meteorites. In: Kerridge, J.F., Matthews, M.S. (Eds.), *Meteorites and the Early Solar System*. Univ. Arizona Press, Tucson, pp. 3–31.

Sears, D.W.G., Grossman, J.N., Melcher, C.L., Ross, L.M., Mills, A.A., 1980. Measuring metamorphic history of unequilibrated ordinary chondrites. *Nature* **287**, 791–795.

Sears, D.W.G., Lyon, I., Saxton, J., Turner, G., 1998. The oxygen isotope properties of olivines in the Semarkona ordinary chondrite. *Meteorit. Planet. Sci.* **33**, 1029–1032.

Sessler, R., Hess, P.C., Rutherford, M.J., 1982. Liquidus relations in the forsterite–silica–anorthite–albite system at 1 atm (abstract). *Lunar Planet. Sci.* **XIII**, 710–711.

Suzuki, A., Yasuda, A., Ozawa, K., 2005. Cr–Al diffusion in chromite spinel at high-pressure (abstract). *EOS Trans. AGU* **86** (52), Fall Meet. Suppl., Abstract V13A-0521.

Tomiyama, T., Yamaguchi, A., Misawa, K., Kojima, H., 2001. Chemical variations of chromites in L-chondrites (abstract). *Symp. Antarct. Meteorites* **XXVI**, 145–146.

Van Schmus, W.R., Wood, J.A., 1967. A chemical-petrologic classification for the chondritic meteorites. *Geochim. Cosmochim. Acta* **31**, 747–765.

Weinbruch, S., Armstrong, J., Palme, H., 1994. Constraints on the thermal history of the Allende parent body as derived from olivine–spinel thermometry and Fe/Mg interdiffusion in olivine. *Geochim. Cosmochim. Acta* **58**, 1019–1030.

Wlotzka, F., 2005. Cr spinel and chromite as petrogenetic indicators in ordinary chondrites: equilibration temperatures of petrologic types 3.7 to 6.. *Meteorit. Planet. Sci.* **40**, 1673–1702.

Yabuki, H., El Goresy, A., Ramdohr, P., 1983. A petrologic microprobe survey of coexisting olivine, pyroxene, and spinels in L- and LL-chondrites (abstract). *Meteoritics* **18**, 426–428.

Zanda, B., Bourot-Denise, M., Perron, C., Hewins, R.H., 1994. Origin and metamorphic redistribution of silicon, chromium, and phosphorus in the metal of chondrites. *Science* **265**, 1846–1849.